Available online at www.sciencedirect.com
ScienceDirect
C. R. Chimie 12 (2009) 1072–1078
COMPTES RENDUS CHIMIE

Full paper / Mémoire

$BaTiO_3$ and $PbTiO_3$ perovskite as catalysts for methane combustion

Ionel Popescu [a], Adriana Urda [a], Tatiana Yuzhakova [b], Ioan-Cezar Marcu [a,*], Jozsef Kovacs [b], Ioan Sandulescu [a]

[a] *Department of Chemical Technology and Catalysis, Faculty of Chemistry, University of Bucharest, 4-12, Blv. Regina Elisabeta, 030018 Bucharest, Romania*
[b] *Department of Environmental Engineering and Chemical Technology, Faculty of Engineering, University of Pannonia, H-8201 Veszprem, Hungary*

Received 27 March 2008; accepted after revision 18 September 2008
Available online 17 November 2008

Abstract

Unsupported and γ-Al_2O_3-supported Ba and Pb titanate catalysts were prepared, characterized and studied in the combustion of methane, as a test reaction for VOCs' catalytic combustion. They present good catalytic activities, and after dispersion (5%) on γ-Al_2O_3 the specific activity of the supported perovskite phase increased 25 and 30 times, respectively, compared with the unsupported samples. $PbTiO_3$/γ-Al_2O_3 shows the best catalytic properties among the tested samples. ***To cite this article: I. Popescu et al., C. R. Chimie 12 (2009).***

Keywords: Ba–Ti perovskite; Pb–Ti perovskite; Catalytic combustion; Methane

1. Introduction

Catalytic combustion is one of the main processes for the destruction of volatile organic compounds (VOCs) [1,2], using either noble metals [3–5] or metal oxides [6,7] as catalysts. Both families of catalysts have been studied extensively for catalytic combustion applications. Although noble metals are the most active catalysts for VOC abatement [8,9], they have some disadvantages like high sintering rates, volatility, poisoning in the presence of water or sulfur compounds and high price [10]. On the other hand, metal oxides have certain advantages, like price, high thermal stability, higher resistance to poisoning and the easy way of preparation, and they appear to be promising materials. Perovskites are extensively studied for this purpose in particular due to their thermal, chemical and structural stability and in many cases improved catalytic activity [11–13]. Furthermore, their dispersion on supports may lead to increased exposed surface areas [14]. In the present work, we report on results obtained in methane catalytic combustion on unsupported and γ-Al_2O_3-supported $BaTiO_3$ and $PbTiO_3$ perovskites. To our knowledge, none of the $BaTiO_3$ and $PbTiO_3$ perovskites has been yet studied as catalysts for methane combustion. The difficulty in

* Corresponding author.
E-mail addresses: marcu.ioan@unibuc.ro, icmarcu@chem.unibuc.ro (I.-C. Marcu).

1631-0748/$ - see front matter © 2008 Académie des sciences. Published by Elsevier Masson SAS. All rights reserved.
doi:10.1016/j.crci.2008.09.006

destroying methane by catalytic combustion, since it is very difficult to activate, makes it a good model compound to test the efficiency of catalysts for VOC combustion, as the catalytic combustion of most organic compounds would be ensured if methane is quantitatively abated.

2. Experimental

2.1. Catalyst preparation

$BaTiO_3$ and $PbTiO_3$ catalysts were prepared from the starting materials $Ba(NO_3)_2$, PbO and TiO_2, through solid state reactions. Raw materials were weighed out in stoichiometric proportion to form the desired composition and mechanically mixed for 1 h. Then the mixtures were calcined in air at 200 and 400 °C for 1 h at each temperature, at 600 °C for 2 h, and, finally, at 1100 °C for 5 h, for $BaTiO_3$ perovskite and at 800 °C for 6 h, for $PbTiO_3$.

The $BaTiO_3/Al_2O_3$ and $PbTiO_3/Al_2O_3$ catalysts, containing 5 wt% perovskite, were obtained by dispersion of $BaTiO_3$ and $PbTiO_3$, respectively, on alumina support. The method of dispersion consists in an original sol–gel process: finely grounded particles of perovskite were added in an aqueous solution of $Al(NO_3)_3$ precursor, followed by precipitation with ammonia under intense stirring, at room temperature, up to a pH equal to 5.5. The obtained samples were dried at 100 °C for 1 h and calcined under air at 200, 400 and 600 °C for 1 h at each temperature, and, finally, at 800 °C for 6 h.

2.2. Catalyst characterization

The samples' structure was investigated by the X-ray diffraction (XRD) method. XRD patterns were recorded with a DRON-2 diffractometer equipped with a Cu Kα source ($\lambda = 1.54$ Å). They were recorded over the 10–70° angular range with a 0.02° step and an acquisition time of 1 s per point.

The analysis of elemental surface compositions of $BaTiO_3$ and $PbTiO_3$ was performed by means of X-ray photoelectron spectroscopy (XPS). XPS spectra were recorded at room temperature and under vacuum of 10^{-9} torr on a VG Scientific ESCA-3 Mk-II spectrometer using monochromatized Al Kα radiation (1486.7 eV). XPS data were analyzed with S_Probe ESCA and XI_SDP32 (XPS International) software programs.

BET specific surface areas of the samples were measured on a Micromeritics ASAP 2020 system under liquid-nitrogen temperature using N_2 adsorption.

The morphology of the samples and the dispersion of perovskites on Al_2O_3 support was investigated using a Philips XL 30 ESEM (Environmental Scanning Electron Microscope) having EDX (Energy Dispersive X-ray) analyzer. An accelerating voltage of 20 kV was used. The powder samples were fixed on a holder and sample compartment was evacuated in order to prevent the electrical charging. Then the surface of particle was photographed and simultaneously quantitative and qualitative electron probe microanalyses were performed. Electron beams were very finely focused. Therefore, elemental analysis of very small area on specimen surface was done in so-called spot mode.

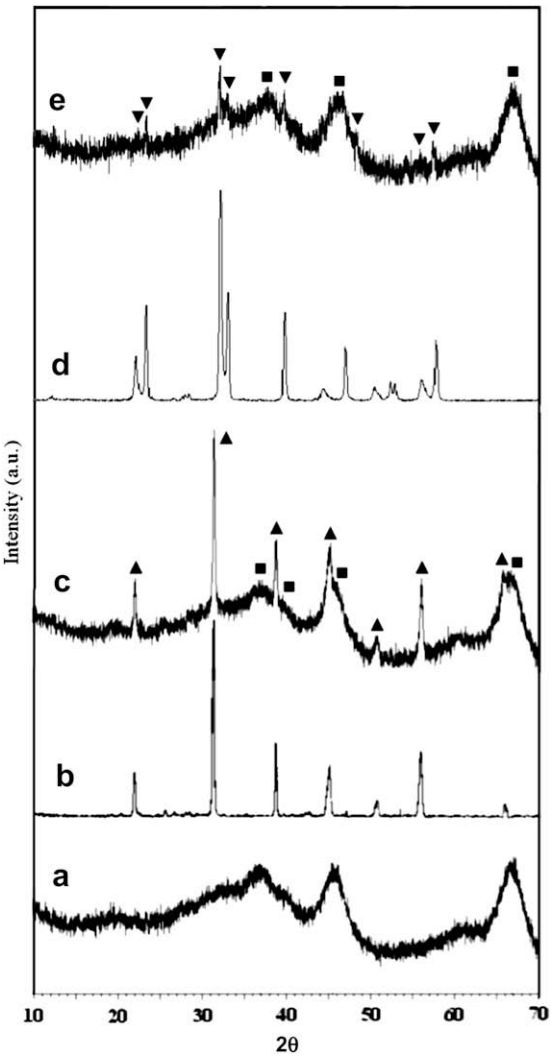

Fig. 1. XRD patterns of the catalysts: a – γ-Al_2O_3, b – $BaTiO_3$, c – $BaTiO_3/Al_2O_3$, d – $PbTiO_3$, e – $PbTiO_3/Al_2O_3$ (■ – γ-Al_2O_3 phase, ▲ – $BaTiO_3$ phase, ▼ – $PbTiO_3$ phase).

Table 1
Textural properties and surface Ti/M atomic ratios of the catalysts (M = Pb or Ba).

Sample	BET surface area (m^2/g)	Average pore diameter (nm)	Pore 4volume (cm^3/g)	XPS surface Ti/M atomic ratio
γ-Al_2O_3	191.0	5.1	0.350	–
$BaTiO_3$	0.4	60.2	0.006	1.1
$BaTiO_3/Al_2O_3$	193.0	4.6	0.350	–
$PbTiO_3$	0.5	15.1	0.002	0.5
$PbTiO_3/Al_2O_3$	175.0	6.4	0.270	–

2.3. Catalytic testing

The combustion of methane was carried out in a fixed bed quartz tube down-flow reactor operated at atmospheric pressure. The internal diameter of the reactor tube was 28 mm. The catalyst was supported by quartz wool. The axial temperature profile was measured using an electronic thermometer placed in a thermowell centered in the catalyst bed. Ceramic rings were used to fill the dead volumes before and after the catalyst bed to minimize potential gas-phase reactions at higher reaction temperatures. The reaction mixture consisted of 5% (vol.) methane in air. Flow rates were controlled by fine needle valves and were measured by capillary flow-meters. The volume hourly space velocity (VHSV) was maintained at 16,000 h^{-1}.

In a typical reaction run, the reactor was heated to the desired temperature in the flow of reactants. The system was allowed to stabilize for about 30 min at the reaction temperature before the first product analysis was made. Each run was carried out over a period of 2–3 h, until two consecutive analyses were identical. The reaction products were analyzed in a Clarus 500 Gas-Chromatograph equipped with a thermal conductivity detector (TCD), using two packed columns in series (6 ft Hayesep and a 10 ft molecular sieve 5 Å).

The conversion was calculated as the amount of raw material transformed in reaction divided by the amount that was fed to the reactor. Complete selectivity to CO_2 and H_2O was always observed.

3. Results and discussion

3.1. Physico-chemical properties of the catalysts

The XRD patterns of the catalysts are displayed in Fig. 1. The alumina support shows the characteristic reflections of γ-Al_2O_3. For $BaTiO_3$ and $PbTiO_3$ samples the XRD patterns indicate only the formation of perovskite phases with tetragonal symmetry, with no

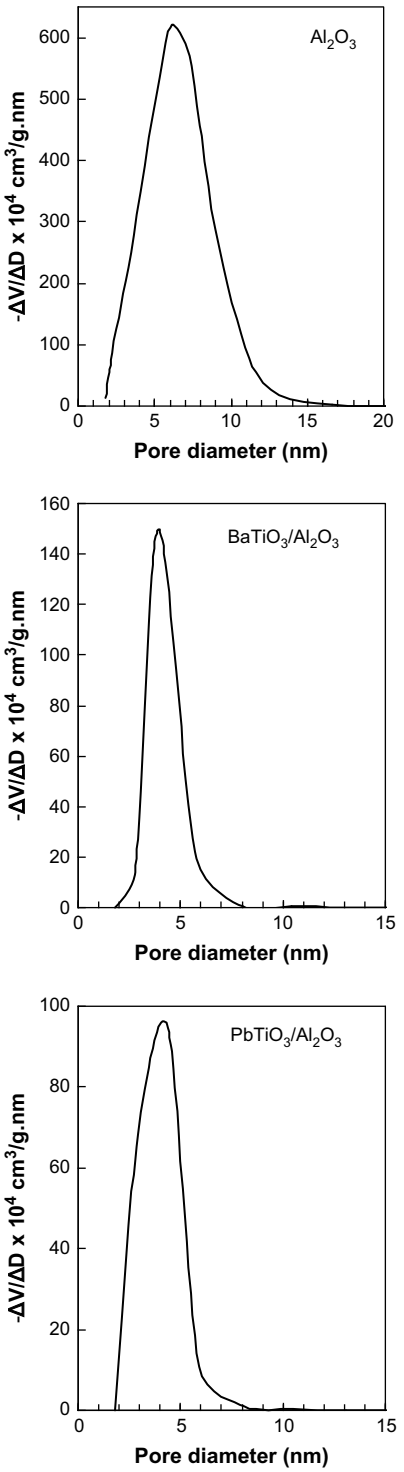

Fig. 2. Pore size distributions of the supported samples and γ-Al_2O_3 support.

other crystalline compounds. After dispersion on γ-Al_2O_3, Ba and Pb titanates maintain their structural integrity. No characteristic peaks corresponding to the $BaAl_2O_4$ and $PbAl_2O_4$ spinel phases were found.

Textural properties of the unsupported and supported perovskites and of the γ-Al_2O_3 support are summarized in Table 1. The specific surface areas of the unsupported perovskites are low, but normal for perovskite-type oxides, especially for those prepared through solid state reaction. At the same time, the specific surface areas of the $BaTiO_3/Al_2O_3$ and $PbTiO_3/Al_2O_3$ systems are very high and similar to γ-Al_2O_3 support. Pore size distributions of the supported samples and γ-Al_2O_3 support are displayed in Fig. 2. They indicate that all the samples show uniform and narrow pore size distribution with average peak pore diameter for both supported samples at 4 nm and for alumina support at 6 nm.

The XPS spectra of bulk $BaTiO_3$ and $PbTiO_3$ samples are displayed in Fig. 3. Surface atomic concentrations of the elements in the investigated samples, presented in Table 1 as surface atomic ratios, were determined from the photoemission peaks areas. The peak corresponding to Ba ($3d_{5/2}$) has two components, as observed by curve fitting, one at about 778.7 eV and another at about 780.6 eV. This indicates the existence of Ba in two different chemical environments at the surface of $BaTiO_3$, related to the ion displacements in the tetragonal structure leading to two types of O^{2-} positions and, consequently, two types of nearest neighbors for Ba^{2+}. This is a characteristic feature of $BaTiO_3$ surfaces [15] associated to ferroelectric domains and c domains, respectively. While for $BaTiO_3$ the surface atomic ratio was roughly equal to the stoichiometric ratio, for $PbTiO_3$ an important superficial excess of lead was observed, but without the segregation of a single lead oxide phase.

The SEM micrographs for $BaTiO_3/Al_2O_3$ and $PbTiO_3/Al_2O_3$ systems are shown in Fig. 4. Islands (bright points) of perovskite with particle size of 1–5 μm covering the alumina surface are observed in both samples. This is confirmed by EDX microprobe analysis focused on ''islands'' and on the support, the results obtained being presented in Table 2. It can be seen that Ti and Ba or Pb content decreases drastically in points S (the support) with respect to the ''islands''. On the other hand, while the Ti/Pb atomic ratio in the $PbTiO_3$ ''islands'' is close to 1, the Ti/Ba atomic ratio in the $BaTiO_3$ ''islands'' is close to 2, suggesting that Ba probably migrates from the perovskite to the alumina support to locally form barium aluminate.

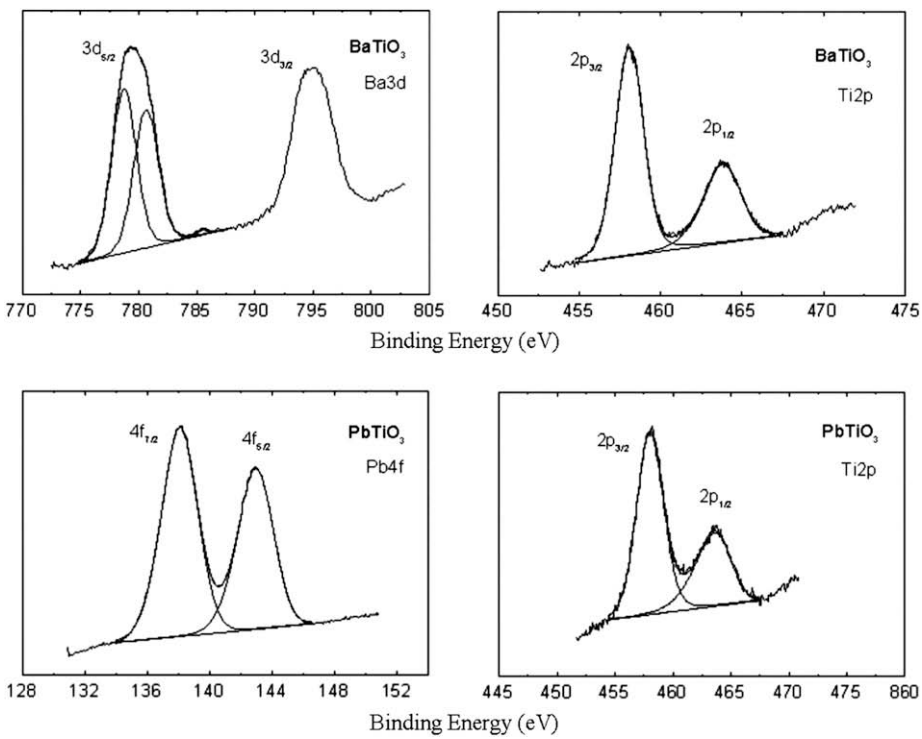

Fig. 3. XPS spectra of unsupported $BaTiO_3$ and $PbTiO_3$ samples.

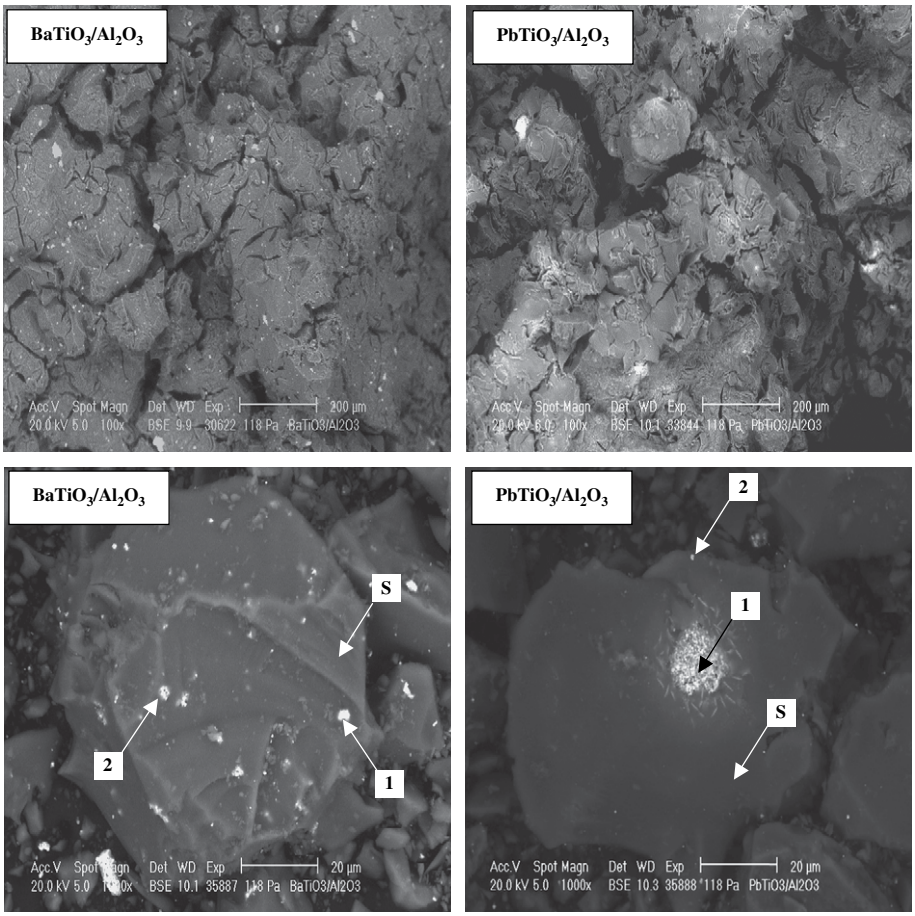

Fig. 4. SEM micrographs of $BaTiO_3/Al_2O_3$ and $PbTiO_3/Al_2O_3$ systems.

3.2. Catalytic properties

The catalytic activities in methane combustion of unsupported and supported perovskites as well as of the alumina support have been determined in the temperature range of 550–800 °C. The only reaction product detected on unsupported and supported perovskites was CO_2, while with γ-Al_2O_3 support

Table 2
EDX microprobe analysis of the supported catalysts in the points indicated in Fig. 4.

Element	Atom % in					
	$BaTiO_3/Al_2O_3$			$PbTiO_3/Al_2O_3$		
	Point 1	Point 2	Point S	Point 1	Point 2	Point S
O	54.2	55.9	61.1	60.7	63.0	54.8
Al	35.5	34.0	38.5	27.3	30.4	43.8
Ti	6.4	7.3	0.3	6.5	2.9	0.5
Ba	3.9	2.8	0.1	–	–	–
Pb	–	–	–	5.5	3.7	0.9

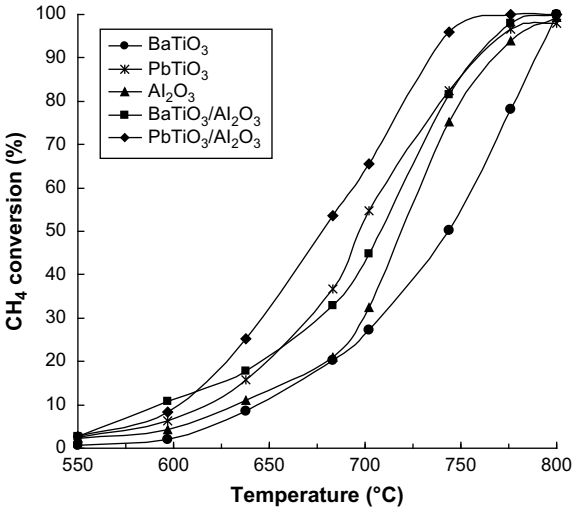

Fig. 5. Methane conversion versus reaction temperature for the five catalysts.

Table 3
Catalytic performances of the catalysts in methane combustion.

Catalyst	T_{50} (°C)	E_a (kcal/mol)	Reaction rate at 700 °C (10^6 mol/g s)	Reaction rate over perovskite phase at 700 °C (10^6 mol/g s)
γ-Al_2O_3	719	29.7	5.57	–
$BaTiO_3$	744	38.1	1.95	1.95
$BaTiO_3/Al_2O_3$	708	27.4	7.69	47.78
$PbTiO_3$	697	31.1	3.94	3.94
$PbTiO_3/Al_2O_3$	678	29.1	11.25	118.98

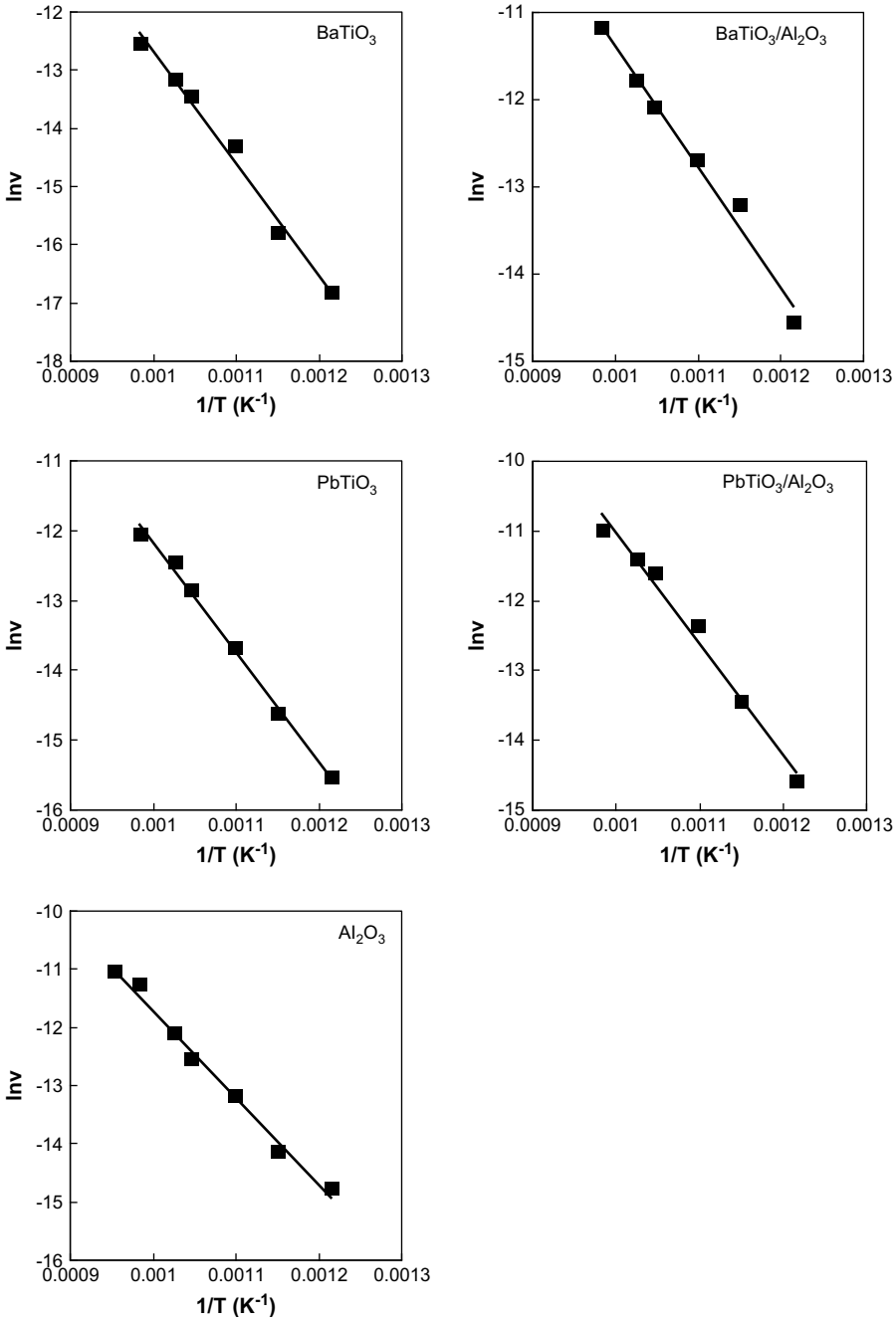

Fig. 6. Arrhenius plots for methane combustion on the five catalysts.

a significant amount of CO was found in the products in line with what was reported in Ref. [16].

The results obtained are shown in Fig. 5, where the measured values of methane conversion are plotted as a function of the reaction temperature. At the same time, the apparent activation energies corresponding to the transformation on the different catalysts have been calculated (Table 3) and the Arrhenius plots obtained (Fig. 6). The values obtained for the activation energies are comparable with those presented in the literature [16]. As clearly shown in Fig. 6 and by values of T_{50} (temperature corresponding to 50% conversion) and of the specific reaction rate in Table 3, unsupported $PbTiO_3$ perovskite is more active than $BaTiO_3$, the last being, surprisingly, less active than alumina. In terms of the specific activity, both perovskites seem to be less active than alumina. This may be due to the very high surface area of alumina compared to unsupported perovskites. On the other hand, both supported catalysts are more active than the corresponding unsupported perovskites, both in terms of T_{50} values and of specific reaction rates. Moreover, an important increase in the reaction rate per unit mass of active component was observed after dispersion of the perovskite phase: 25 times for $BaTiO_3/\gamma$-Al_2O_3 and 30 times for $PbTiO_3/\gamma$-Al_2O_3 compared with the unsupported perovskite phases. At the same time, even though a decrease of the apparent activation energy was observed for the supported catalysts, it was insignificant for $PbTiO_3$ perovskite. These observations suggest that dispersion of perovskites on γ-Al_2O_3 results in an increased exposed surface area of the active component, responsible for the observed increase of the catalytic activity.

We note that the specific activity of the supported perovskite phase (the active component) in the supported catalyst, a, was calculated from the difference between the overall specific activity of the supported catalyst, a_1, and the specific activity of alumina support, a_0, as follows:

$$a = (a_1 - 0.95a_0)/0.05$$

where 0.95 and 0.05 are factors corresponding to the alumina and perovskite content in the supported catalyst, respectively.

4. Conclusion

$BaTiO_3$ and $PbTiO_3$ perovskites have been obtained by means of the solid state reaction method. The catalysts are single perovskite phases with an important surface enrichment in lead for $PbTiO_3$. They exhibit good activity in methane catalytic combustion, $BaTiO_3$ being less active than $PbTiO_3$. Perovskites were supported on γ-Al_2O_3 by incorporation of perovskite powders in the alumina support during its precipitation. From the structural point of view no formation of new phases has been detected after dispersion. Dispersion of perovskites on γ-Al_2O_3 results in an increase of the catalytic activity due to the increasing of the exposed surface area.

Acknowledgements

The authors are grateful to Mr. Oravetz Dezső for his expertise and for technical assistance with scanning electron micrographs recording and EDX analysis.

References

[1] P. Thevenin, G. Menon, S. Järäs, CATTECH 7 (1) (2003) 10.
[2] D. Ciuparu, M.R. Lyobovsky, E. Altman, L.D. Pfefferle, A. Datye, Catal. Rev. 44 (4) (2002) 593.
[3] P. Gelin, M. Primet, Appl. Catal. B 39 (2002) 1.
[4] T.V. Choudhary, S. Banerjee, V.R. Choudhary, Appl. Catal. A 234 (2002) 1.
[5] K. Narui, K. Furuta, H. Yata, A. Nishida, Y. Kohtoku, T. Matsuzaki, Catal. Today 45 (1998) 173.
[6] Y. Moro-oka, W. Ueda, K.H. Lee, J. Mol. Catal. A: Chem. 199 (2003) 139.
[7] A.J. Zarur, J.Y. Ying, Nature 403 (2000) 65.
[8] K. Foger, H. Jaeger, J. Catal. 120 (1989) 465.
[9] R.A. Dalla Betta, Catal. Today 35 (1997) 129.
[10] R.M. Heck, R.J. Farrauto, Catalytic Air Pollution Control: Commercial Technology, Van Nostrand Reinhold, New York, 1995.
[11] L.G. Tejuca, J.L.G. Fierro, J.M.D. Tascon, Adv. Catal. 35 (1989) 237.
[12] L. Fabrini, A. Kryukov, S. Capelli, G.L. Chiarello, I. Rosetti, C. Oliva, L. Forni, J. Catal. 232 (2005) 247.
[13] I. Popescu, I.C. Marcu, I. Sandulescu, D. Macovei, Prog. Catal. 15 (2006) 79.
[14] M. Alifanti, M. Florea, V. Cortes-Corberan, U. Endruschat, B. Delmon, V.I. Parvulescu, Catal. Today 112 (2006) 169.
[15] S. Kumar, V.S. Raju, T.R.N. Kutty, Appl. Surf. Sci. 206 (2003) 250.
[16] S. Cimino, L. Lisi, R. Pirone, G. Russo, M. Turco, Catal. Today 59 (2000) 19.